AIP Journal of Applied Physics

High-frequency properties of oriented hcp-$Co_{1-x}Ir_x$ ($0.06 \le x \le 0.24$) soft magnetic films

Fei Xu, Sha Zhang, Dezheng Yang, Tao Wang, and Fashen Li

Citation: Journal of Applied Physics **117**, 17B725 (2015); doi: 10.1063/1.4916933
View online: http://dx.doi.org/10.1063/1.4916933
View Table of Contents: http://scitation.aip.org/content/aip/journal/jap/117/17?ver=pdfcov
Published by the AIP Publishing

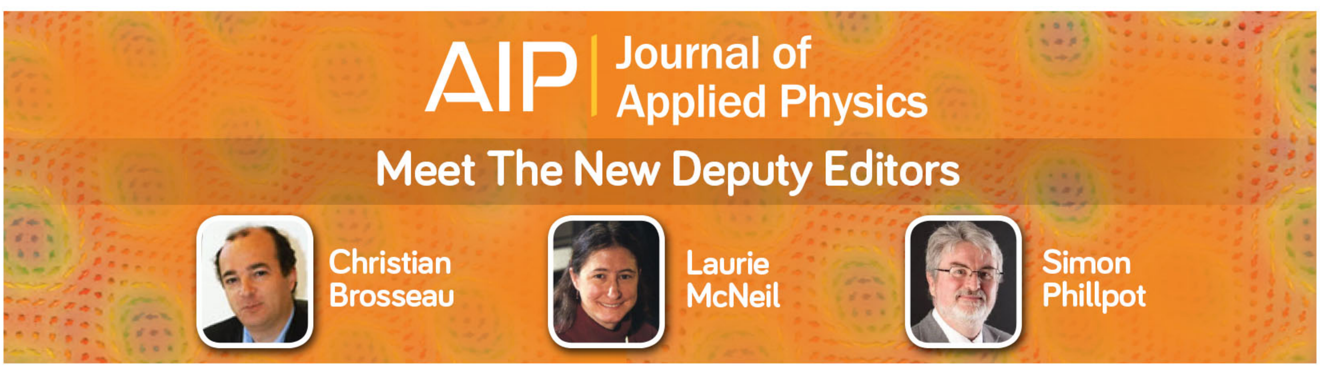

JOURNAL OF APPLIED PHYSICS **117**, 17B725 (2015)

High-frequency properties of oriented hcp-$Co_{1-x}Ir_x$ ($0.06 \le x \le 0.24$) soft magnetic films

Fei Xu, Sha Zhang, Dezheng Yang, Tao Wang,[a)] and Fashen Li
Key Laboratory of Magnetism and Magnetic Materials of Ministry of Education, Lanzhou University, Lanzhou 730000, China

(Presented 4 November 2014; received 21 September 2014; accepted 23 November 2014; published online 3 April 2015)

In this work, the composition dependence of high-frequency magnetic properties for the oriented *hcp*-$Co_{1-x}Ir_x$ soft magnetic films with negative uniaxial magnetocrystalline anisotropy (K_u^{grain}) and in-plane uniaxial anisotropy field (H_u) is investigated. Both the saturation magnetization (M_s), K_u^{grain}, and H_u are greatly affected by the composition of Ir. The $(\mu_i - 1) \cdot f_r$ of $Co_{1-x}Ir_x$ (with negative K_u^{grain}) is larger than Acher's limit (without K_u^{grain}) when x exceeds 0.14. The increasing percent of $(\mu_i - 1) \cdot f_r$ could get a maximum of 42% when x is 0.2. © *2015 AIP Publishing LLC*.
[http://dx.doi.org/10.1063/1.4916933]

I. INTRODUCTION

As a traditional magnetic material, Co with hcp crystal structure exhibits positive uniaxial magnetocrystalline anisotropy along its c-axis. However, there are many works which indicate that CoIr alloy with hcp structure shows strong negative uniaxial magnetocrystalline anisotropy (K_u^{grain}) with the doping of Ir.[1–5] In this case, the easy magnetization direction is along c-plane or perpendicular to c-axis. In the reported literature on CoIr, most of their works focused on the static magnetic properties for potential application of soft underlayer in magnetic recording.[1,4,5] With the development of information technology and electromagnetic devices, the application of high-frequency soft magnetic films becomes more and more extensive, such as microwave absorber, micro-inductor, micro-transformer, and magnetic head with high writing speed.[6–10] Recently, CoIr film has a great application prospect for high-frequency application due to its novel high-frequency magnetic properties with negative K_u^{grain}.[11,12]

For a soft magnetic film without considering magnetocrystalline anisotropy and with in-plane anisotropy (H_u) which satisfies $H_u \ll 4\pi M_s$, the natural resonance frequency f_r and the initial permeability μ_i are described as

$$\mu_i = 1 + 4\pi M_s/H_u, \tag{1}$$

$$f_r = \gamma/2\pi\sqrt{4\pi M_s H_u}. \tag{2}$$

Equation (2) is named by the Kittel formula. We can see that the increase of natural resonance frequency can only be accomplished by reducing μ_i for a certain material with a fixed M_s through increasing H_u. As reported by Wang *et al.*,[11,12] CoIr films with negative K_u^{grain} can solve the above problem. After the introduction of the negative K_u^{grain} ($H_u^{grain} = -2K_u^{grain}/M_s$), f_r and μ_i could be expressed as

$$\mu_i = 1 + 4\pi M_s/H_u, \tag{3}$$

$$f_r = \frac{\gamma}{2\pi}\sqrt{(4\pi M_s + H_u^{grain})H_u}. \tag{4}$$

The natural resonance frequency can be increased by introduction of H_u^{grain}, while the μ_i is still determined by $4\pi M_s/H_u$. The reported work has shown that K_u^{grain} remains negative value in a large range of Ir.[1,2] In this paper, we systematically investigate the composition dependence of high-frequency magnetic properties for soft $Co_{1-x}Ir_x$ by varying the content of Ir.

II. EXPERIMENT

Ta, Pt, Ru, Co, and Ir targets are used to fabricate the films by using magnetron sputtering system. The Si (001) wafers with surface oxidation are used as the substrate. The base pressure of the vacuum is smaller than 5.0×10^{-5} Pa, the sputter pressure is 0.4 Pa for Pt, 0.15 for Ru and Ta, and 0.11 Pa for CoIr layers. The layered structure of the samples is substrate/Ta (9 nm)/Pt (10 nm)/Ru (13 nm)/$Co_{1-x}Ir_x$ (140 nm)/Ru (4 nm). The in-plane uniaxial anisotropy of the films is induced by the oblique sputtering. The Surface profile-meter (Dektak 8) is used to determine the thickness of the films. The film's composition is measured by Atomic emission spectrometer (ICP). The X-ray diffraction technique (XRD, Philips X'Pert PRO with Cu K_α radiation, Holland) is used to characterize the crystalline structure.[13] The static magnetic properties are characterized by vibrating sample magnetometer (VSM). The FMR measurements are performed in an X band VARIAN spectrometer. The cavity resonance frequency is 9.0 GHz. Agilent E8363B vector network analyzer with a shorted microstrip method is used to characterize the high-frequency magnetic properties.[14]

III. RESULTS AND DISCUSSION

The composition dependence of XRD pattern of the CoIr films is shown in Fig. 1. We can see that there are only four peaks, which are (1 1 1) peak of Pt, (0 0 2) peak of Ru, a strong (0 0 2) peak of $Co_{1-x}Ir_x$, and a very weak (101)

a)Author to whom correspondence should be addressed. Electronic mail: wtao@lzu.edu.cn.

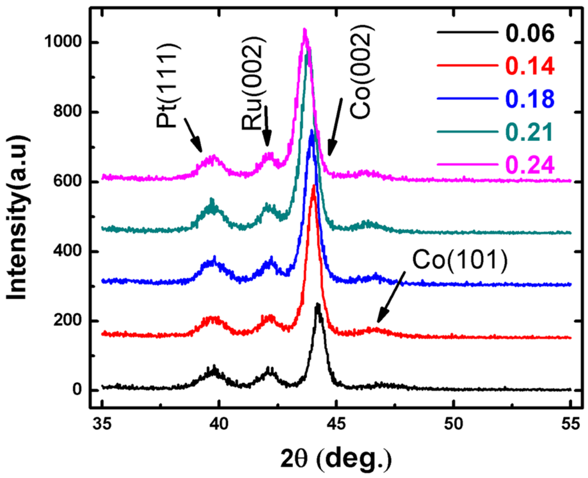

FIG. 1. The composition dependence of XRD pattern for the $Co_{1-x}Ir_x$ films.

peak of $Co_{1-x}Ir_x$. For each sample, the oriented (0 0 2) hcp-Ru grows on the (1 1 1) plane of Pt, and then the oriented $Co_{1-x}Ir_x$ film is gotten. From the (002) and (101) peak of the $Co_{1-x}Ir_x$, we can see that I_{002}/I_{101} is higher than 21 in the range of $0.06 \leq x \leq 0.24$. It reveals that the oriented hcp-$Co_{1-x}Ir_x$ films with c-axis perpendicular to the film plane are successfully realized. From the figure, we could also see that there is a significant left-drift of the (0 0 2) peak of $Co_{1-x}Ir_x$ with the increase of Ir. The diffraction angle 2θ reduces from 44.2° to 43.6° as x increases from 0.06 to 0.24. As the atomic diameter of the Ir is bigger than Co, the lattice constant of the CoIr becomes bigger with the increase of Ir. Thus, the left-drift of the (0 0 2) peak of $Co_{1-x}Ir_x$ indicates that Ir is successfully doped in hcp Co.

The typical in-plane hysteresis loops of $Co_{1-x}Ir_x$ films with $x = 0.14$ and 0.21 are displayed in Fig. 2(a). The magnetic field applied in the film plane is parallel and perpendicular to the easy axis, respectively. It is clear that all the films have soft magnetic properties and obvious in-plane uniaxial anisotropy. The magnetic parameters of all $Co_{1-x}Ir_x$ ($0.06 \leq x \leq 0.24$) films obtained from the hysteresis loops are shown in Fig. 2(b). The $4\pi M_s$ has an obvious change with increasing x, and reduces from 17.85 KGs to 10.96 KGs. This is ascribed to the increasing of non-magnetic Ir per unit volume. When x is larger than 0.24, the $4\pi M_s$ of the films will become smaller and the magnetocrystalline anisotropy will become weak, so the upper limit of x is fixed as 0.24. Additionally, the easy axis coercivity (H_{ce}) increases abruptly with increasing x.

In this work, the in-plane uniaxial anisotropy field (H_u) and the total out-of-plane anisotropy field ($H_\theta = 4\pi M_s + H_u^{grain}$) are achieved via azimuth angle dependence of ferromagnetic resonance field ($H_r(\varphi)$). All the resonance fields (H_r) are measured with the microwave magnetic field and applied magnetic field in film plane. The relationship between the resonance field and the in-plane angle from Ref. 15 is

$$\left(\frac{\omega}{\gamma}\right)^2 = (\boldsymbol{H}_\mathbf{r}(\cos(\varphi_\mathbf{h} - \varphi_\mathbf{m}) + \boldsymbol{H}_\mathbf{u}\cos^2(\varphi_\mathbf{m}) + \boldsymbol{H}_\theta) \times (\boldsymbol{H}_\mathbf{r}(\cos(\varphi_\mathbf{h} - \varphi_\mathbf{m}) + \boldsymbol{H}_\mathbf{u}\cos(2\varphi_\mathbf{m}))|_{\varphi_\mathbf{m}=\varphi_0}. \tag{5}$$

Here, φ_0 is the equilibrium positions of the magnetization, while φ_h is the angle between applied magnetic field and the easy axis. The experimental data for the film with $x = 0.14$ are shown in Fig. 3(a) as black dots. When the applied magnetic field and the easy axis are parallel to each other, the resonance field is smallest, while when perpendicular the largest value is gotten. As a function of the azimuth angle, $H_r(\varphi)$ displays a well-defined in-plane uniaxial symmetry. The fitted result by using Eq. (5) is shown in Fig. 3(a) as a red line. The experimental and fitted results agree well with each other. All the fabricated films are measured in this way, and the H_u and H_θ are extracted by the fitted results. The H_u of the films is shown in Fig. 2(b). It increases with increasing x. From the picture, we could see that the easy axis coercivity (H_{ce}) and the in-plane uniaxial anisotropy field (H_u) have the same tendency with increasing x. In our work, the fabrication conditions are the same for all films. Thus, we could explain the tendency of H_{ce} via the in-plane uniaxial anisotropy dependence of the easy axis coercivity model, in which H_{ce} is proportional to H_u. Meanwhile, the H_θ of the films is shown in Fig. 3(b). It increases first and then reduces with the increase of x. Since H_θ is expressed as $4\pi M_s + H_u^{grain}$, H_u^{grain} is extracted by $H_\theta - 4\pi M_s$ and also shown in Fig. 3(b). It increases with the increase of x. The calculated K_u^{grain} from $K_u^{grain} = -M_s H_u^{grain}/2$ is listed in Table I.

For traditional soft magnetic films without considering magnetocrystalline anisotropy, we can get the natural resonance frequency (f_r^{Kittel}) and the initial permeability (μ_i) via Eqs. (1) and (2), the values of μ_i and f_r^{Kittel} are shown in Table I. When the negative K_u^{grain} is introduced in CoIr film,

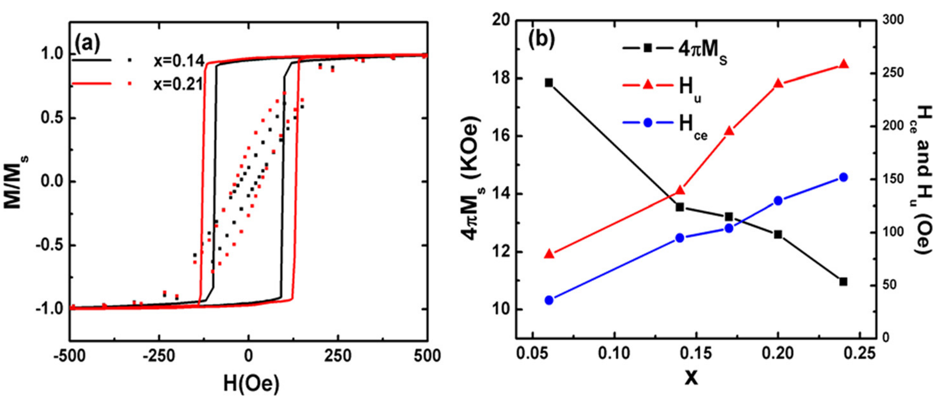

FIG. 2. (a) The hysteresis loops along easy axes (solid lines) and hard axes (dotted lines) of $Co_{1-x}Ir_x$ films with $x = 0.14$, 0.21, (b) the composition dependence of $4\pi M_s$, H_{ce}, and H_u for $Co_{1-x}Ir_x$ films.

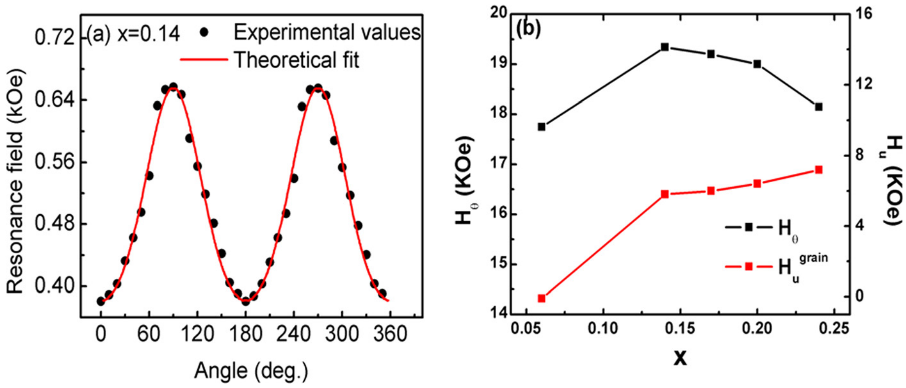

FIG. 3. (a) The resonance field dependence of angle between the applied field and the easy axis for x = 0.14 film. The dots are experimental data and the curve is the fitted result. (b) The composition dependence of H_θ and H_u^{grain} for $Co_{1-x}Ir_x$ films.

TABLE I. Parameters of $Co_{1-x}Ir_x$ films with various x.

x	K_u^{grain} ($\times 10^6$ erg/cm^3)	μ_i	f_r^{cal} (GHz)	f_r^{Kittel} (GHz)	f_r^{exp} (GHz)
0.06	0.07	218.68293	3.93	3.32	2.56
0.14	−3.13	125.40678	4.59	3.84	4.67
0.17	−3.15	76.64246	5.42	4.49	5.41
0.20	−3.21	92.73611	5.98	4.87	5.58
0.24	−3.14	81.76923	6.06	4.71	6.08

the μ_i and f_r^{cal} calculated by Eqs. (3) and (4) are also shown in Table I. From Table I, we can see that the initial permeability does not change via Eqs. (1) and (3). It reduces with the increasing of Ir because of the decreasing of $4\pi M_s$ and the increasing of H_u. However, f_r^{cal} is much higher than f_r^{Kittel} for the introduction of negative K_u^{grain} when x is larger than 0.06. When x is 0.06, the K_u^{grain} of $Co_{1-x}Ir_x$ films is positive, leading to $H_\theta < 4\pi M_s$. Thus, f_r^{cal} is smaller than f_r^{Kittel} when x is 0.06.

The complex permeability spectra of $Co_{1-x}Ir_x$ films with different x are measured by vector network analyzer. The typical complex permeability spectra of $Co_{1-x}Ir_x$ films with x = 0.06 and 0.14 are displayed in Figs. 4(a) and 4(b), where μ' and μ'' represent the real and imaginary parts of complex permeability, respectively. The natural resonance frequency (f_r^{exp}) of all $Co_{1-x}Ir_x$ ($0.06 \le x \le 0.24$) films obtained from the complex permeability spectra is shown in Fig. 5(a). We can see that the calculated f_r^{cal} by using Eq. (4) agrees well with the measured resonance frequency f_r^{exp} when x > 0.14. However, f_r^{exp} is obviously smaller then the f_r^{cal} at x = 0.06. When x is 0.06, the K_u^{grain} of $Co_{1-x}Ir_x$ films is positive. In this case, the c-axis of CoIr film turns into the easy axis, so the total out-of-plane anisotropy is smaller than the demagnetization field $4\pi M_s$. Additionally, the local moments might not strictly lie in the film any longer due to the easy-axis of CoIr grains being perpendicular to the film plane. In this situation, the calculation formula of natural resonance frequency for soft magnetic film may be not suitable, which leads to f_r^{exp} being smaller than f_r^{cal}.

The product of the susceptibility and the natural frequency of the soft magnetic film is expressed as $(\mu_i - 1)\cdot f_r = 2\gamma M_s\sqrt{H_\theta/H_u}$. For traditional soft magnetic film without considering magnetocrystalline anisotropy, H_θ only contains $4\pi M_s$. Hence, the above formula is transformed into $(\mu_i - 1)\cdot f_r = 2\gamma M_s\sqrt{4\pi M_s/H_u}$, which can be obtained by Acher's limit. The calculated results by using $4\pi M_s$ and H_u of $Co_{1-x}Ir_x$ are listed in Fig. 5(b). For the oriented $Co_{1-x}Ir_x$ film with negative K_u^{grain}, H_θ is the summation of $4\pi M_s$ and H_u^{grain}. Therefore, the above formula is transformed into $(\mu_i - 1)\cdot f_r = 2\gamma M_s\sqrt{(4\pi M_s + H_u^{grain})/H_u}$. The results are also listed in Fig. 5(b). We can see that the product of $(\mu_i - 1)\cdot f_r$ for CoIr film is dramatically larger than that of traditional soft magnetic film with the same M_s, but without considering magnetocrystalline anisotropy. Here, we use the increasing percent of $(\mu_i - 1)\cdot f_r$ to identify the contribution from the H_u^{grain}. The increasing percent (P) is expressed as

$$p = \frac{100\left(2\gamma M_s\sqrt{(4\pi M_s + H_u^{grain})/H_u} - 2\gamma M_s\sqrt{4\pi M_s/H_u}\right)}{2\gamma M_s\sqrt{4\pi M_s/H_u}}\%.$$

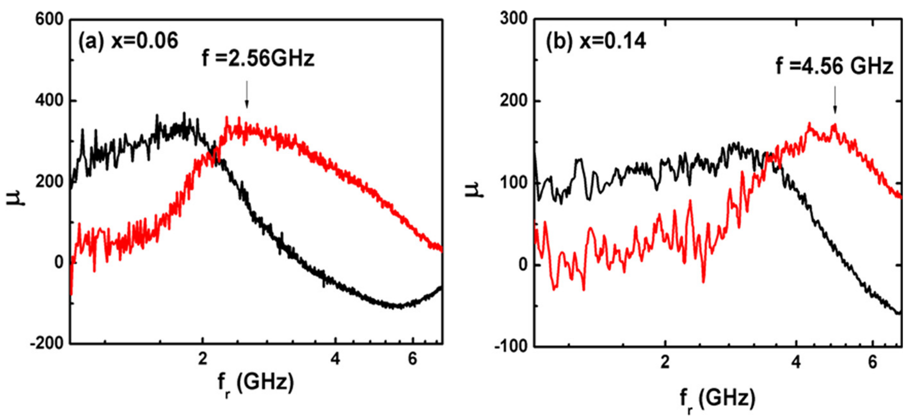

FIG. 4. The complex permeability spectra of $Co_{1-x}Ir_x$ films with different x (a) x = 0.06, (b) x = 0.14.

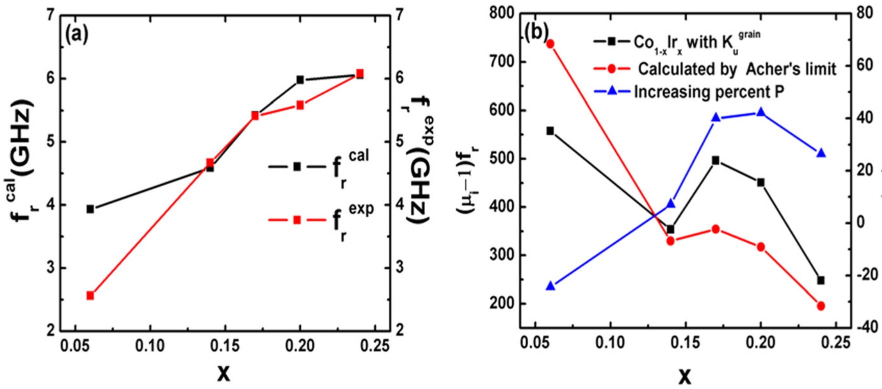

FIG. 5. (a) The composition dependence of f_r^{exp} and f_r^{cal} for $Co_{1-x}Ir_x$ films. (b) The Acher's limit and P of $Co_{1-x}Ir_x$ films with different x.

The value of P of all $Co_{1-x}Ir_x$ films is shown in Fig. 5(b). We can see that the value increases initially, then reduces with the increasing x. It gets the biggest value of 42% when x is 0.2.

IV. CONCLUSION

We systematically investigate the composition dependence of high-frequency magnetic properties for oriented soft $Co_{1-x}Ir_x$ films by varying the content of Ir. When K_u^{grain} is negative, the measured natural resonance frequency is obviously larger than that calculated by Kittel formula. As the initial permeability is still determined by $4\pi M_s/H_u$, the $(\mu_i - 1)\cdot f_r$ is much larger than Acher's limit, and the increasing percent gets the biggest value of 42% when x is 0.2.

ACKNOWLEDGMENTS

This work was supported by the National Natural Science Foundation of China, Nos. 11204115 and 11144008, National Basic Research Program of China, No. 2012CB933101, and Fundamental Research Funds for the Central Universities, No. lzujbky-2013-22.

[1] A. Hashimoto, S. Saito, and M. Takahashi, J. Appl. Phys. **99**, 08Q907 (2006).
[2] D. Hasegawa, S. Nakasaka, M. Sato, T. Ogawa, and M. Takahashi, IEEE Trans. Magn. **42**, 2805 (2006).
[3] C. N. Chinnasamy, T. Ogawa, D. Hasegawa, H. T. Yang, S. D. Yoon, V. G. Harris, and M. Takahashi, IEEE Trans. Magn. **43**, 3112 (2007).
[4] N. Nozawa, S. Saito, T. Kimura, K. Shibuya, K. Hoshino, S. Hinata, and M. Takahashi, Appl. Phys. Lett. **102**, 012407 (2013).
[5] S. Park, J. G. Zhu, and D. E. Laughlin, J. Appl. Phys. **105**, 07B723 (2009).
[6] V. Hari Babu, J. Rajeswari, S. Venkatesh, and G. Markandeyulu, J. Magn. Magn. Mater. **339**, 1 (2013).
[7] V. Georgescu and M. Dau, Surf. Sci. **600**, 4195 (2006).
[8] A. Hashimoto, S. Ito, and S. Nakagaw, J. Magn. Magn. Mater. **310**, 2636 (2007).
[9] Z. Y. Zhong, H. W. Zhang, Y. L. Jing, X. L. Tang, L. Zhang, and S. Liu, Vacuum **82**, 491 (2008).
[10] K. Hirat, A. Hashimoto, T. Matsuu, and S. Nakagaw, Mater. Sci. Eng., B **161**, 134 (2009).
[11] T. Wang, Y. Wang, G. G. Tan, F. S. Li, and S. J. Ishio, Physica B **417**, 24 (2013).
[12] S. Zhang, F. Xu, X. M. Ma, T. Wang, G. G. Tan, and F. S. Li, Appl. Surf. Sci. **299**, 81 (2014).
[13] D. W. Guo, X. L. Fan, G. Z. Chai, C. J. Jiang, X. L. Li, and D. S. Xue, Appl. Surf. Sci. **256**, 2319 (2010).
[14] D. W. Guo, C. J. Jiang, X. L. Fan, H. G. Shi, and D. S. Xue, Appl. Surf. Sci. **258**, 4237 (2012).
[15] M. Farle, Rep. Prog. Phys. **61**, 755 (1998).